(12) Kratohvil, P. *J. Polym. Sci., Polym. Symp.* **1975**, *No. 50*, 487.
(13) Huglin, M. B.; Richards, R. W. *Polymer* **1976**, *17*, 588.
(14) Chu, B.; Gulari, Es. *Macromolecules* **1979**, *12*, 445.
(15) DiNapoli, A.; Chu, B.; Cha, C. *Macromolecules* **1982**, *15*, 1174.
(16) Chu, B.; Lee, D.-C. *Macromolecules* **1984**, *17*, 926.
(17) Ford, J. R.; Chu, B. "Proceedings of the 5th International Conference on Photon Correlation Techniques in Fluid Mechanics"; Schulz-Dubois, E. O., Ed.; Springer-Verlag: New York, 1983; pp 303–314.
(18) Stockmayer, W. H.; Schmidt, M. *Pure Appl. Chem.* **1982**, *54*, 407.
(19) Shuely, W., private communication.
(20) See: Huglin, M. B. In "Light Scattering from Polymer Solutions"; Huglin, M. B., Ed.; Academic Press: New York, 1972; p 184.
(21) Koppel, D. E. *J. Chem. Phys.* **1972**, *57*, 4814.
(22) ter Meer, H. U.; Burchard, W.; Wunderlich, W. *Colloid Polym. Sci.* **1980**, *258*, 675.

X-ray Scattering from Polythiophene: Crystallinity and Crystallographic Structure

Z. Mo, K.-B. Lee, Y. B. Moon, M. Kobayashi, A. J. Heeger, and F. Wudl*

Department of Physics, Institute for Polymers and Organic Solids, University of California, Santa Barbara, California 93106. *Received February 13, 1985*

ABSTRACT: X-ray scattering has been used to investigate the crystallinity and crystal structure of chemically coupled polythiophene. Heat treatment at elevated temperatures leads to significant increases in crystallinity (from ~35% as synthesized up to ~56% after annealing at 380 °C for 30 min) and coherence length indicative of chain growth and extension. Chemical analysis of the chain-extended polythiophene shows a major reduction in residual iodine content consistent with growth of the polymer chains to approximately 1200 thiophene rings. An initial model of the crystal structure of polythiophene is presented.

Introduction

Polythiophene (PT) can be viewed as an sp^2p_z carbon chain in a structure (see Figure 1) somewhat analogous to that of *cis*-$(CH)_x$ but stabilized in that structure by the sulfur, which covalently bonds to neighboring carbons to form the heterocycle.[1] Conjugated polymers such as polythiophene are of current interest since they are semiconductors that can be doped, with resulting electronic properties that cover the full range from insulator to metal.[2] Moreover, the polyheterocycles are of specific theoretical interest since the two valence bond configurations sketched in Figure 1b are not energetically equivalent.[3] As a result, the inherent coupling of electronic excitations to chain distortions in such linear conjugated polymers leads to the formation of polarons and bipolarons as the dominant species involved in charge storage and charge transport.

High-quality polythiophene has recently been synthesized by chemical coupling of 2,5-diiodothiophene.[1] On the basis of chemical analysis of the residual iodine content, the chemically prepared polythiophene consists of polymer chains with approximately 45 thiophene rings (~180 carbon atoms along the backbone). This chemically coupled polythiophene contains a relatively small concentration of unpaired spins and a clean IR spectrum, indicative of a stereoregular polymer with a relatively high degree of structural perfection. Moreover, preliminary X-ray scans showed that the polymer is crystalline.[4]

Photoexcitation of neutral PT leads to photogeneration of polarons with associated changes in the visible–IR absorption spectrum and with photoinduced ESR.[5] In situ studies[3] of PT during electrochemical doping have demonstrated that in the dilute regime, charge is stored in bipolarons, weakly confined soliton pairs with a confinement parameter $\gamma \simeq 0.1$–0.2. After doping to saturation with AsF_5 (~24 mol %), the electrical conductivity increases by nearly 10 orders of magnitude[1] to 14 Ω^{-1} cm^{-1}. Moreover, the optical properties,[3] the magnitude and temperature dependence of the thermopower,[1] and the existence of a temperature-independent Pauli spin susceptibility[6] all indicate a truly metallic state for the heavily doped polymer.

Table I
Chemical Composition of Polythiophene (%)

M_r	C	H	S	I	remarks
3958[a]	56.71	2.63	37.05	3.17	as synthesized
	58.67	2.40	39.24	0.13	after annealing at 300 °C
98700	58.43	2.45	38.99	0.13	calcd

[a] 49 ppm Mg and 51 ppm Ni were also present in this sample.

In this paper, we focus on an X-ray scattering investigation of the crystallinity and crystallographic structure of chemically coupled PT. We find that heat treatment at 300 °C for 30 min leads to significant increases in crystallinity (from ~35% as synthesized up to ~52%) and coherence length indicative of chain growth and extension. This is accompanied by loss of iodine; chemical analysis of the chain-extended PT shows a major reduction in residual iodine content consistent with growth of polymer chains to approximately 1200 thiophene rings, or a molecular weight of $\sim 10^5$. From analysis of the powder pattern Bragg diffraction, we have obtained crystallographic data that allow indexing and identification of the unit cell parameters. Based upon one-to-one similarities with the *d* spacings found for poly(*p*-phenylene), an initial model of the structure is presented with two polythiophene chains in the unit cell.

Experimental Techniques

The polythiophene used in these experiments was synthesized by condensation polymerization of 2,5-diiodothiophene as described earlier.[1] The composition (as obtained from chemical analysis) of the as-synthesized polymer is given in Table I. The dark brown powder was packed into an aluminum mold (0.80 in. × 0.40 in × 0.12 in) for heat treatment and subsequent X-ray scattering measurements.

The X-ray scattering apparatus utilizes a Huber 430/440 goniometer, which allows independent horizontal rotations of the sample and the detector with angular resolution of 0.001°. The Cu K_α radiation was provided by a 1-kW Philips X-ray tube (40 kV at 25 mA). As monochromator and analyzer we used flat HOPG crystals. Powder scans were obtained from the as-synthesized polymer and from the same sample after annealing in dry N_2 at 200, 250, 300, and 380 °C for 30 min. In a separate series of experiments, the heat treatment was carried out with the sample in air.

0024-9297/85/2218-1972$01.50/0

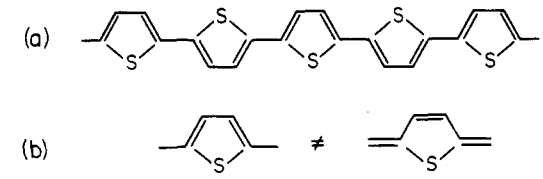

Figure 1. (a) Chemical structure diagram of polythiophene. (b) Two inequivalent structures for the thiophene heterocycle in polythiophene.

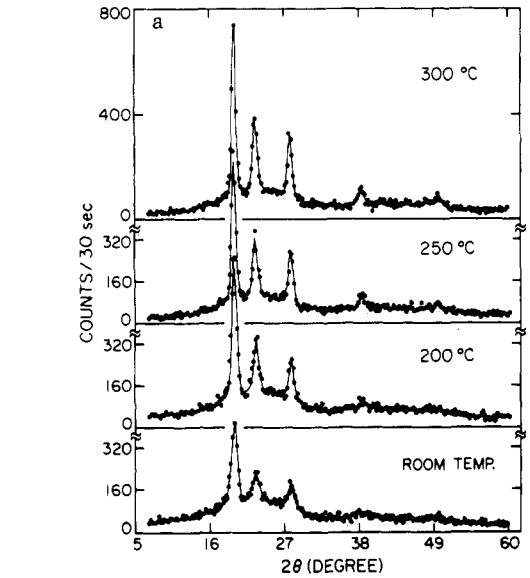

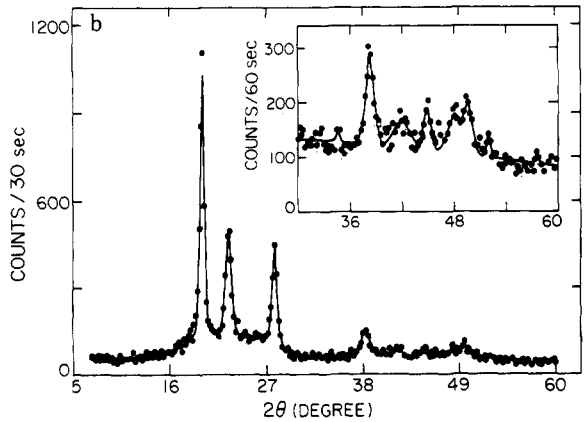

Figure 2. (a) X-ray powder diffraction curves for polythiophene after heat treatment at indicated temperatures for 30 min. (b) X-ray powder diffraction curve for polythiophene after heat treatment at 380 °C for 30 min.

Experimental Results

The powder pattern scans are plotted in Figure 2a for a single sample that was heat treated in dry nitrogen. In a separate experiment, a different sample was heat treated at 380 °C (Figure 2b). The solid curves drawn through the data points in Figure 2 represent a least-squares fitting function composed of a sum of Gaussians. For example, to describe the data after the 300 °C anneal, the fitting function consisted of five narrow Gaussian peaks for the sharp Bragg reflections and two broad Gaussians for the diffuse background. These are better resolved in Figure 2b, where 11 lines can be observed. Thus, the scattered intensity from the crystalline regions, $I_{cr}(\theta)$, is represented by the five narrow Gaussians, whereas the total scattered intensity, $I_t(\theta)$ is represented by the full sum of seven Gaussians. Similar fits were constructed for each data set. Since the fits are in all cases excellent, the fitting functions are used for the quantitative analysis described in the following section. The best fits to the data obtained from the as-synthesized sample and the same sample after the 300 °C anneal are compared directly in Figure 3.

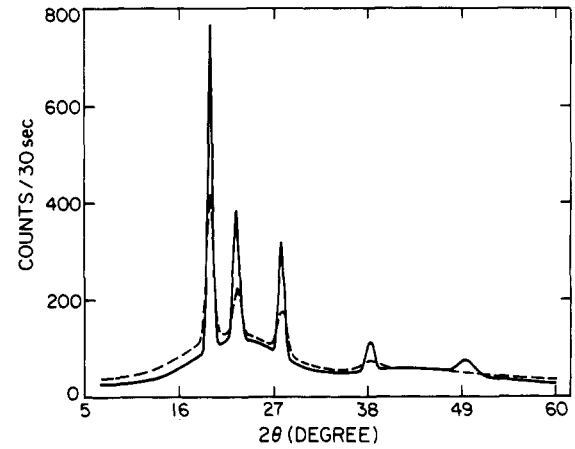

Figure 3. Comparison of best fits to the scattering data of Figure 2 from the as-synthesized material (dashed curve) and from the same sample after annealing at 300 °C for 30 min (solid curve).

Table II
X-ray Data for the Strongest Crystalline Reflection of PT Powder

specimen treatment[a]	2θ, deg	corr height of peak	half-width
room temp	19.65	300	0.96
473 K, 30 min	19.64	520	0.82
523 K, 30 min	19.63	525	0.73
573 K, 30 min	19.62	671	0.66

[a] Under N_2.

The effects of heat treatment are evident in Figures 2 and 3: (i) The Bragg peaks are successively narrower after annealing at higher temperatures. (ii) The integrated area under the Bragg peaks increases after annealing at higher temperature. (iii) The diffuse scattering background decreases after annealing at higher temperatures. We find, furthermore, that the widths of the Bragg peaks are consistently slightly narrower if the sample is cooled slowly subsequent to the anneal (rather than quenched rapidly to room temperature). These changes imply an increase in the volume fraction of the sample that is crystalline and an improvement in the coherence length (i.e., the perfection) of the crystalline regions. Detailed analysis of the data (see following section) confirms the increase in crystallinity and crystallite coherence and provides quantitative measures of the relevant parameters.

The X-ray data for the strongest crystalline Bragg reflection obtained after annealing under N_2 are summarized and compared in Table II. The three improvements noted above are obtained for samples annealed either in air or under N_2. The excellent stability of polythiophene in air at elevated temperatures is of particular interest.

Ruland Analysis of the Crystallinity

The crystallinity of polythiophene as synthesized and after heat treatment was determined by the Ruland method.[7,8] The volume fraction of the sample that is crystalline, X_{cr}, is defined as follows:

$$X_{cr} = \frac{\int_0^\infty q^2 I_{cr}(q)\, dq}{K \int_0^\infty q^2 I_t(q)\, dq} \qquad (1)$$

where $I_{cr}(q)$ is the intensity under the Bragg peaks, $I_t(q)$

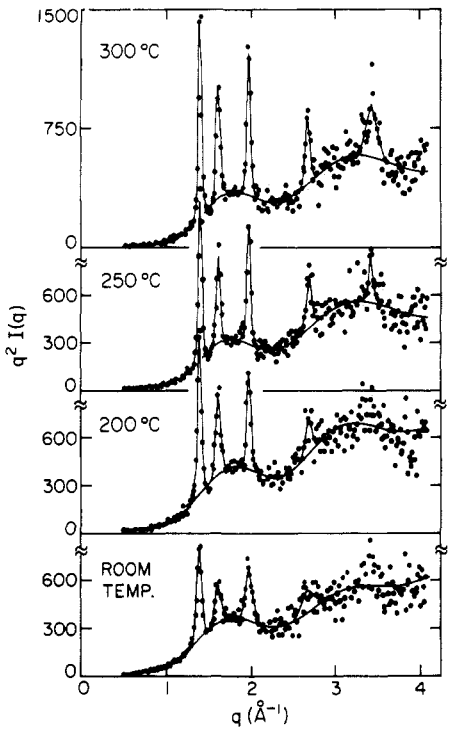

Figure 4. X-ray powder diffraction intensity curve $q^2I(q)$ for polythiophene after heat treatment at indicated temperatures.

is the total scattered intensity (Bragg peaks plus diffuse background), and q is the magnitude of the scattering vector, $q = 4\pi(\sin\theta)/\lambda$. The correction factor, K, is a weighted Debye–Waller factor

$$K = \frac{\int_0^\infty q^2\langle f^2\rangle e^{-kq^2}\,dq}{\int_0^\infty q^2\langle f^2\rangle\,dq} \tag{2}$$

where

$$\langle f^2\rangle = \Sigma N_i f_i^2/\Sigma N_i \tag{3}$$

is the weighted mean square atomic form factor of the polymer, $f_i(q)$ is the form factor of an atom of type i, and N_i is the number of such atoms (per monomer). The imperfection factor, k, arises since thermal motion and lattice imperfection cause part of the X-ray intensity scattered from the crystalline region to appear in the diffuse background.

Equations 1 and 2 give

$$X_{cr} = \left[\frac{\int_0^\infty q^2 I_{cr}(q)\,dq}{\int_0^\infty q^2 I_t(q)\,dq}\right]\left[\frac{\int_0^\infty q^2\langle f^2\rangle\,dq}{\int_0^\infty q^2\langle f^2\rangle e^{-kq^2}\,dq}\right] \tag{4}$$

The finite range in 2θ (and in q) of the experimental data necessarily limits the integration range from $2\theta = 7°$ ($q_1 \simeq 0.45 \times 10^8$ cm^{-1}) to $2\theta = 60°$ ($q_{max} \simeq 4.1 \times 10^8$ cm^{-1}). Nevertheless, the crystallinity can be estimated with reasonable accuracy by the limited-range integrals of eq 5

$$X_{cr} = K(k)^{-1}\frac{\int_{q_1}^{q_2} q^2 I_{cr}(q)\,dq}{\int_{q_1}^{q_2} q^2 I_t(q)\,dq} \tag{5}$$

For fixed q_1, if q_2 is large enough, the inferred crystallinity will be independent of q_2. As a procedure, therefore, the best value of X_{cr} is determined by varying the disorder parameter (k), computing X_{cr} as a function of the upper limit (q_2), and finding the value of k that yields a constant X_{cr}, i.e. independent of q_2.

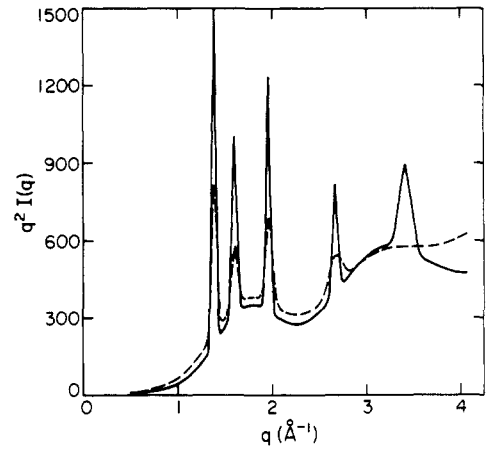

Figure 5. Comparison of best fits to $q^2I(q)$ data of Figure 4 from the as-synthesized sample and from the same sample after annealing at 300 °C for 30 min.

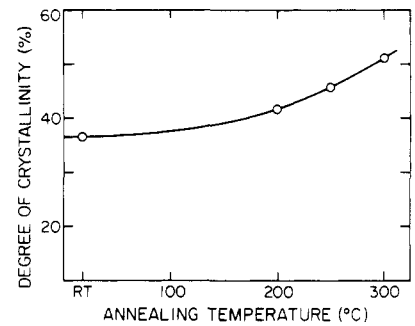

Figure 6. Variation of X_{cr} in PT as a function of heat treatment temperature (under N_2).

The data of Figure 2 are replotted as $q^2I_t(q)$ vs. q in Figure 4. After correction for polarization, this total intensity was resolved (using the fitting function) into the background diffuse scattering contribution and the crystalline diffraction contribution, $q^2I_{cr}(q)$. The $q^2I_t(q)$ plots for the as-synthesized sample and for the same sample after annealing at 300 °C are compared directly in Figure 5. The effect of the heat treatment is clearly evident.

The crystallinity values were obtained through application of eq 5; the results are summarized in Table III. Examination of Table III shows that for $k = 0.05 \times 10^{-16}$ to 0.075×10^{-16} cm^2 reasonably constant values are obtained for the crystallinity independent of the upper limit (q_2) of the integral. Although the precise value of X_{cr} depends on the choice of the best k, the trend is clear and unambiguous; the crystallinity increases upon annealing from values of about 35% for the as-synthesized material to values of about 55% after the 300 °C anneal. Rewriting the effective Debye–Waller factor as $\exp(-kq^2) \equiv \exp(-{}^1/_3\langle u^2\rangle q^2)$ reveals that this range of k corresponds to average root mean square displacements from the perfect lattice (in the crystalline regions) of $\langle u^2\rangle^{1/2} \simeq 0.3$–$0.5$ Å. After the anneal at 380 °C, the Ruland analysis yields a value for $X_{cr} \simeq 0.56$ with k somewhat reduced ($k \simeq 0.05 \times 10^{-16}$ cm^2), consistent with improved order in the crystalline regions. The coherence length (after 380 °C heat treatment) increased to $\xi \simeq 174$ Å.

The resulting values for X_{cr} (with $k = 0.076 \times 10^{-16}$ cm^2) are plotted in Figure 6 as a function of the heat treatment temperature. The annealing procedure causes a clear and

Table III
Crystallinity of PT as a Function of k and Integration Interval[a]

room temp						250 °C					
	$4\pi^2k$, Å^2						$4\pi^2k$, Å^2				
$q_2/2\pi$	0	2	3	4	5	$q_2/2\pi$	0	2	3	4	5
0.65	19.9	32.0	39.8	48.9	59.4	0.65	23.0	37.1	46.1	56.7	68.9
0.54	22.0	30.6	34.9	41.7	48.3	0.54	25.3	35.2	41.2	48.0	55.5
0.49	24.2	32.2	36.9	42.1	47.8	0.49	28.8	38.2	43.8	50.0	56.8
0.45	27.1	34.5	38.7	43.3	48.4	0.45	23.6	42.7	47.9	53.6	59.9
0.41	25.9	31.6	34.8	38.3	42.0	0.41	34.4	42.0	46.3	50.8	55.8
0.37	28.1	33.0	35.7	38.6	41.6	0.37	38.7	45.4	49.2	53.1	57.3
0.30	27.6	29.1	32.5	34.3	38.1	0.30	37.8	42.7	44.5	47.0	49.5
0.28	32.7	36.1	37.8	39.6	41.4	0.28	44.3	48.7	51.0	53.5	56.0
			36.5[b]						46.3[b]		
200 °C						300 °C					
	$4\pi^2k$, Å^2						$4\pi^2k$, Å^2				
$q_2/2\pi$	0	2	3	4	5	$q_2/2\pi$	0	2	3	4	5
0.65	20.9	33.7	41.9	51.5	62.6	0.65	28.7	46.2	57.5	70.7	85.9
0.54	23.2	32.4	37.9	44.1	51.1	0.54	29.1	40.6	47.5	55.3	64.0
0.49	26.1	34.7	39.7	45.3	51.5	0.49	31.6	42.0	48.1	54.9	62.4
0.45	30.1	38.2	42.9	48.1	53.6	0.45	36.4	46.3	52.0	58.2	60.0
0.41	31.1	37.9	41.8	45.9	50.4	0.41	37.1	45.2	50.0	54.7	60.8
0.37	34.5	40.5	43.8	47.3	51.0	0.37	41.1	48.2	52.2	56.3	54.8
0.30	36.3	40.5	42.7	45.1	47.5	0.30	41.8	46.7	49.3	52.0	61.8
0.28	42.7	47.0	49.2	51.5	54.0	0.28	48.9	53.8	56.4	59.1	67.6
			42.5[b]						51.6[b]		

[a] See eq 5. $q_1/2\pi = 0.07$. [b] Average value.

unambiguous increase in the crystallinity from $X_{cr} = 0.37$ for the as-synthesized polymer to $X_{cr} = 0.52$ after annealing at 300 °C for 30 min (either under dry nitrogen or in air). This increase in crystallinity is accompanied by a narrowing of the diffraction peaks and by an increase in the observable number of diffraction peaks. For example, one sees only three Bragg peaks for the as-synthesized polymer, whereas there are five clearly observable Bragg peaks after annealing at 300 °C.

The narrowing of the diffraction peaks (see Figure 2, Figure 4, and Table II) implies an increase in the coherence length (or crystallite size) as a result of the elevated temperature anneal. Under the assumption that all the line broadening results from finite crystallite size, the coherence length (in Å) was calculated from the Sherrer equation[9]

$$\xi = 57.3\lambda/(\beta \cos \theta)$$

where $\beta = (B^2 - b_0^2)^{1/2}$, B is the measured half-width of the experimental profile (in degrees), b_0 is the instrumental resolution (in degrees), λ is the wavelength of the X-radiation, and 2θ is the scattering angle. The instrumental resolution, obtained from scans of single-crystal silicon, was found to be 0.2°. Using the data of Table II for the strongest crystalline reflection, we have plotted in Figure 7 the calculated coherence length as a function of annealing temperature.

The increased crystallinity and crystalline coherence that results from the high-temperature heat treatment arise from a combination of two effects: chain extension by oligomer–oligomer reaction and improved chain–chain lateral packing resulting from increased chain mobility at elevated temperatures. The principal evidence indicating chain extension comes from chemical analysis. Evolution of iodine was observed during the annealing period. Since the chemical coupling of 2,5-diiodothiophene necessarily leaves an iodine atom at the chain end, the iodine content is a direct indicator of molecular weight. To quantify the loss of iodine, the 300 °C anneal was repeated for chemical analysis with the sample in dynamic vacuum (the material that evolved was trapped in the vacuum line). The chemical analysis results from the annealed material are

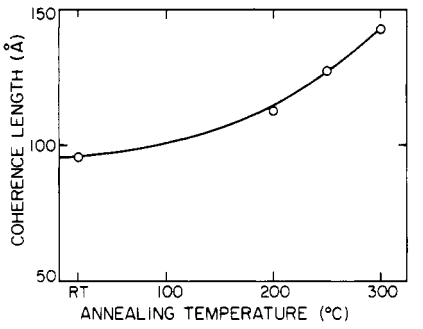

Figure 7. Variation of coherence length (from the width of the most intense reflection, Table II) as a function of the heat treatment temperature (annealed under N_2).

included for comparison in Table I. The residual iodine content decreased from 3.17% (as synthesized) to 0.13% after heat treatment at 300 °C. Assuming all of the residual iodine is covalently bonded at the chain ends, the heat-treated polythiophene has undergone significant chain extension to an average of approximately 1200 thiophene rings or a molecular weight of $\sim 10^5$.

In spite of the significant improvements that result from the highest temperature (380 °C) anneal, the resulting polymer is only $\simeq$56% crystalline, and the crystalline regions are imperfect with mean square deviation from the perfect lattice sites of approximately 0.3 Å. Thus, although annealing leads to significant improvement, the resulting polythiophene material is far from the complete ideal crystalline equilibrium. Although exposure to higher temperature for extended periods of time might be expected to lead to further improvement, the onset of polymer degradation sets a practical upper limit of $\sim$380 °C (under N_2) as indicated by the thermogravimetric analysis (TGA) data of Figure 8. The weight loss at 380 °C is approximately 7 wt %, i.e., greater than the change in iodine content as determined by elemental analysis. Thus, in addition to chain extension some evolution of short oligomers must be involved. This was confirmed by analysis of the IR spectrum of the trapped material, which

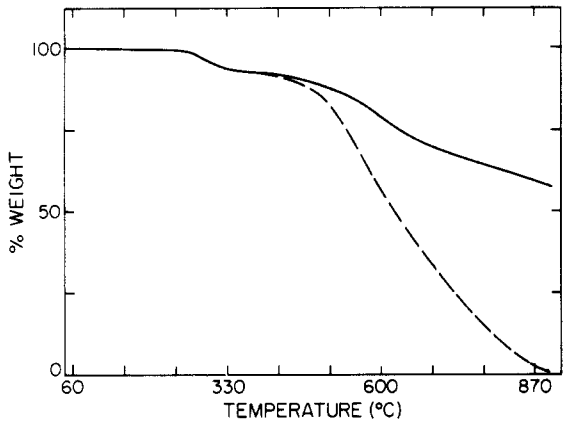

Figure 8. Thermogravimetric analysis (TGA) of polythiophene: solid curve, under N_2; dashed curve, in air.

showed the presence of thiophene rings.

Crystallographic Data: Unit Cell Parameters and Model of the Structure

Table IV lists the observed d spacings corresponding to the crystalline reflections of polythiophene. Although the lattice constants cannot be unambiguously determined with these few reflections, we have attempted to index the unit cell using the data from related systems as a guide. The corresponding data[10] from poly(p-phenylene) are therefore listed for comparison in Table IV. The one-to-one correspondence in the observed d spacings implies a similar crystal structure and similar chain packing for the two systems. This implies an individual chain structure for polythiophene in which the thiophene units alternate as shown in Figure 1. Such an alternating structure is generally accepted for polyheterocycles and results in a straight-chain conformation. The alternative chain structure (with the rings oriented with sulfur atoms always on one side) would lead to significant curvature of the polymer chain requiring a spiral conformation and a crystal structure very different from that of poly(p-phenylene).

In an attempt to construct a model of the crystal structure of a polymer a principal requirement is that the chain structure must be compatible with the crystal structure into which the chains are packed. Thus, for a conjugated polymer, the rigid backbone and the requirement of invariance after translation by a lattice constant provide strict constrains on the possible chain directions in a unit cell.

With these constraints and with the use of the indices of poly(p-phenylene) as a guide, we are able to index the observed reflections by assuming two models: (a) an orthorhombic unit cell with a = 7.80 Å, b = 5.55 Å, and c = 8.03 Å (the calculated and observed d spacings (and the line indices) are given in Table IVa) and (b) a monoclinic unit cell with a = 7.83 Å, b = 5.55 Å, c = 8.20 Å, and β = 96° (the calculated and observed d spacings (and the line indices) are given in Table IVb).

Table IV lists the d spacings and indices for poly(p-phenylene) for comparison. We note that dithiophene has a monoclinic structure[12] with lattice parameters a = 7.76 Å, b = 5.90 Å, c = 8.91 Å, and β = 106.6°.

The value for c can be estimated from the known chemical structure of the thiophene monomer. With the assumption of 120° bond angles and standard carbon–carbon bond lengths for the pseudopolyene backbone (see Figure 1), the repeat unit is approximately 8.5 Å. On the other hand, a repeat unit of approximately 7.8 Å is obtained from analysis of the minimum-energy configuration for quaterthiophene.[11] Thus, we conclude 7.8 Å < c < 8.5 Å, consistent with the values listed in Table IV.

Table IV
X-ray Diffraction Data for Polythiophene

	d, Å			poly(p-phenylene)[10]	
2θ, deg	obsd	calcd	Miller indices	d, Å	Miller indices
		(a) Orthorhombic Unit Cell[a]			
19.73	4.500	4.522	110	4.525	110
22.74	3.910	3.900	200	3.910	200
27.98	3.189	3.191	210	3.190	210
34.60	2.593[c]	2.614	120	2.600[d]	120
38.28	2.351	2.354	310	2.354	310
41.92	2.155[c]	2.176	221 (213)		
44.98	2.015[c]	2.008	004	2.096	002
48.24	1.887[c]	1.897	320	1.890[d]	320
49.57	1.839	1.840	410	1.830[d]	410
52.03	1.760[c]	1.768	313		
		1.756	131		
		1.754	402		
57.60	1.600[c]	1.595	420	1.590[d]	420
		(b) Monoclinic Unit Cell[b]			
19.73	4.500	4.520	110	4.525	110
22.74	3.910	3.894	200	3.910	200
27.98	3.189	3.187	210	3.190	210
34.60	2.593[c]	2.614	120	2.600[d]	120
38.28	2.351	2.351	310	2.354	310
41.92	2.155[c]	2.162	213		
		2.166	$\bar{1}22$		
44.98	2.015[c]	2.039	004	2.096	022
48.24	1.887[c]	1.896	320	1.890[d]	320
49.57	1.839	1.837	410	1.830[d]	410
52.03	1.760[c]	1.767	131		
		1.755	$\bar{4}11$		
57.60	1.600[c]	1.594	420	1.590[d]	420

[a] a = 7.80 Å, b = 5.55 Å, c = 8.03 Å, β = 90°, ρ = 1.567 g/cm^3. [b] a = 7.83 Å, b = 5.55 Å, c = 8.20 Å, β = 96°, ρ = 1.537 g/cm^3. [c] Very weak reflection observed on slow scans with 60 s per point. [d] Very weak reflection (see ref 10).

With the above lattice parameters, the calculated density is approximately 1.55 g/cm^3 (see Table IV), assuming two chains per unit cell. The preliminary result of a density measurement (with no attempt to correct for porosity) of the as-synthesized sample is 1.21 g/cm^3, in satisfactory agreement with the calculation since the density of the partially amorphous material is expected to be less than that of the fully crystalline polymer. The measured density together with the crystallographic data does establish the existence of two chains per unit cell.

Conclusions

Heat treatment of polythiophene leads to a significant increase in the crystallinity and to the improvement of coherence within the crystalline regions. The chain growth and extension is implied by the structural data and confirmed by chemical analysis. After 30 min of annealing at 300 °C, the residual iodine content is consistent with growth of the polythiophene chains to approximately 1200 thiophene units or a molecular weight of nearly 10^5.

Although the crystallographic data are incomplete, they do lead to an initial model of the structure of polythiophene. The results are consistent with an orthorhombic unit cell with lattice constants a = 7.80 Å, b = 5.55 Å, and c = 8.03 Å or a monoclinic unit cell with a = 7.83 Å, b = 5.55 Å, c = 8.20 Å, and β = 96°. In either case, the polymer axis is along c, and there are two polymer chains per unit cell. More detailed information on the chain packing and the precise determination of the monoclinic angle β will require a more detailed analysis based upon an enlarged data set from polythiophene of even higher crystallinity.

Acknowledgment. This study was principally supported by a grant from the Office of Naval Research. M.K. was supported by Showa Denko K.K. We thank H. Yoshida of Showa Denko K.K. for sending us the preliminary powder pattern results on polythiophene.

References and Notes

(1) Kobayashi, M.; Chen, J.; Chung, T.-C.; Moraes, F.; Heeger, A. J.; Wudl, F. *Synth. Met.* **1984**, *9*, 77–86.
(2) (a) Diaz, A. *Chem. Scr.* **1981**, *17*, 145. (b) Tourillon, G.; Garnier, F. *J. Electroanal. Chem.* **1982**, *135*, 173. (c) Yamamoto, T.; Sanechika, K.; Yamamoto, A. *J. Polym. Sci., Polym. Lett. Ed.* **1980**, *18*, 9. (d) Lin, J. W.-P.; Dudek, L. P.; *J. Polym. Sci., Polym. Chem. Ed.* **1980**, *18*, 2869. (e) Kossmehl, C.; Chatzithedorou, G. *Makromol. Chem., Rapid Commun.* **1981**, *2*, 551. (f) Bargon, J.; Mohmand, S.; Waltman, R. J.; *IBM J. Res. Dev.* **1983**, *27*, 330. (g) Kaneto, K.; Kohno, Y.; Yoshino, K.; Inuishi, Y. *J. Chem. Soc., Chem. Commun.* **1983**, 382.
(3) Chung, T.-C.; Kaufman, J. H.; Heeger, A. J.; Wudl, F. *Phys. Rev. B: Condens. Matter* **1983**, *30*, 702–710.
(4) Yoshida, H.; Taneaki, N., private communication.
(5) Moraes, F.; Schaffer, H.; Kobayashi, M.; Heeger, A. J.; Wuld, F. *Phys. Rev. B: Condens. Matter* **1984**, *30*, 2948.
(6) Moraes, F.; Davidov, D.; Kobayashi, M.; Chung, T.-C.; Chen, J.; Heeger, A. J.; Wudl, F. *Synth. Met.*, in press.
(7) Ruland, W. *Acta Cyrstallogr.* **1961**, *14*, 1180; *Polymer* **1964**, *5*, 89.
(8) Akaishi, T.; Miyasaka, K.; Ishikawa, K.; Shirakawa, H.; Ikeda, S. *J. Polym. Sci., Polym. Phys. Ed.* **1980**, *18*, 745–750.
(9) Alexander, L. E. "X-Ray Diffraction Methods in Polymer Science"; Wiley-Interscience: New York, 1976; Chapter 7.
(10) Kovacic, P.; Feldman, M. B.; Kovovacic, J. P.; Lando, J. B. *J. Appl. Polym. Sci.* **1968**, *12*, 1735.
(11) Bredas, J. L.; Themans, B.; Fripiat, J. G.; Andre, J. M.; Chance, R. R. *Phys. Rev B: Condens. Matter* **1984**, *29*, 6761.
(12) Visser, G. J.; Heeres, G. J.; Walters, J.; Vos, A. *Acta Crystallogr. B: Struct. Crystallogr. Cryst. Chem.* **1968**, *24*, 467.

Qualitative Evaluation of the Band Gap in Polymers with Extended π Systems

Olof Wennerström

Department of Organic Chemistry, Chalmers University of Technology, S-412 96 Göteborg, Sweden. *Received January 3, 1985*

ABSTRACT: Hückel calculations combined with C_m-symmetry transformations have been used for a qualitative evaluation of the frontier orbital gap (band gap) in a series of hypothetical polymers containing a polyacetylene skeleton. Similarly, the band gaps in polymers with pyrrole rings and related species have been calculated.

Recently we demonstrated a facile method based on Hückel theory and symmetry properties for the evaluation of a lower limit for the band gap (energy difference between filled and empty MO:s) in a series of polyarenes and poly(vinylarenes).[1] The linear polymer chains are regarded as being similar to a large cyclic polymer, and a C_m-symmetry transformation of the total Hückel determinant results in a series of smaller ones, the majority of which represent degenerate MO:s. However, the series also includes a determinant that can be derived from the smallest repetitive unit closed upon itself to form a ring of Hückel topology and, if n is even, another determinant that can be derived from the same ring but with Möbius topology. The important frontier orbitals that correspond to the band gap in the polymer can usually be found within either of the two subsets of MO energies derived from the two smallest rings of different topology. This result is shown schematically in Figure 1.

In this paper the scheme for the evaluation of the lower limit of the frontier orbital gap (band gap) has been applied to a series of hypothetical and idealized polymers with special emphasis on modified polyacetylenes and nitrogen-containing species with the aim to identify polymers with small band gaps, a property of prime importance for possible applications of the polymers as organic conductors.

Results and Discussion

Polyacetylene (PA) is by far the most studied organic conductor with a large delocalized π system.[2] By the simple Hückel approximation the band gap should ideally be zero; i.e., the frontier orbitals are two degenerate nonbonding orbitals with two electrons, as in the case of [4n]annulenes. However, bond alternation raises the degeneracy of the frontier orbitals to give a finite value for the band gap, $2|\beta_1 - \beta_2|$, where β_1 and β_2 are the resonance integrals for the double and single bonds.[3] By use of bond lengths for [4n]annulenes and a β value of 2.2 eV calculated from electrochemical data, a lower limit for the band gap in PA of 1.0 eV (exptl 1.4 eV, ref 2e) was calculated.[1b] To make the calculations as simple as possible here I have assumed a constant resonance integral for the hydrocarbons and slightly modified coloumb and resonance integrals for the heteroatoms and their bonds to carbon atoms.[4a]

The calculated lower limits of the band gap relative to that of PA for a series of polymers and some related ring compounds are collected in Table I.

Hydrocarbon Chains. If α-, β-, and γ-bridging vinylene groups are introduced into the carbon chain in polyacetylene, three new polymers, **3**, **4**, and **5**, respectively, will result. Of these, the poly(3,4′-fulvalene) (**4**) has the same small band gap ($\Delta = 0.0\beta$) as PA by this method, whereas the band gaps in the hypothetical poly(1,2-cyclobutadienylene) and the well-known poly(*p*-phenylene)[2c,d] are much larger ($\Delta = 0.76\beta$ and 0.83β, respectively). Upon incorporation of an increasing number of sp^2 carbon atoms between the five-membered rings in polymer **4** to give **6**, **7** and **8**, an interesting alternation of the band gap is revealed by the HMO calculations. For the series of β-bridged polyacetylenes **4**, **6**, **7**, and **8**, the first and the third have the same calculated band gap as PA, whereas the second and the fourth members have band gaps of $\Delta = 0.62\beta$ and 0.45β, respectively. A similar alternating behavior is observed for the three polymers **5**, **9**, and **14** with conjugated six-membered rings separated by none, one, and two sp^2 carbon atoms, respectively, although in this case the first and third members have the larger band gaps, $\Delta = 0.83\beta$ and 0.51β, respectively. The intermediate polymer **9** has the same band gap as PA. It

0024-9297/85/2218-1977$01.50/0